

Correlation Coefficient and Loading Effects for MIMO Antennas in a Reverberation Chamber

Nick Janssen^{1,2}, Kate A. Remley²,
Christopher L. Holloway², William F. Young²

¹Electromagnetics Group, Technical University Eindhoven, 5612AZ Eindhoven, The Netherlands

²National Institute of Standards and Technology, Boulder, CO USA

email: kate.remley@nist.gov, phone:303-497-3652

Abstract—We explore the effect of loading a reverberation chamber on the calculation of the correlation coefficient of two-element antenna arrays (similar to the type used in multiple-input multiple-output (MIMO) wireless devices). The changes in correlation coefficient with loading are compared to the changes in a squared, mismatch-corrected version of the transmission coefficient $\langle |S_{xy}|^2 \rangle$ as a function of chamber loading. The correlation coefficient and corresponding coefficient of variation were not significantly different for the unloaded versus loaded measurements as compared to the S parameter metric. The results presented here indicate that since the correlation coefficient is for the most part independent of loading, characterizing the spatial uniformity of the chamber would not be useful. On the other hand, loading a chamber in order to match a real-world environment will not affect the measured correlation between antennas, which is crucial in the performance evaluation of MIMO systems.

Index Terms—bi-monopole antenna, coefficient of variation, correlation coefficient, K-factor, MIMO, reverberation chamber, spatial uniformity, wireless system

I. INTRODUCTIONS

In the last several years, advances have been made in the area of multiple-input, multiple-output (MIMO) antenna performance measurements in both anechoic chambers (ACs) and more recently in reverberation chambers (RCs) [1, 2]. Some of the research on reverberation chambers (RCs) was focused on how to perform measurements and use the different parameters to specify the characteristics of MIMO systems. Parameters considered include, capacity [3, 4, 5], diversity gain [5, 6], efficiency [7], the Rician K-factor [8], and bit-error-rate (BER) [9, 10, 11, 12]. All these parameters are useful in communication systems; e.g., machine-to-machine communication, modern telecommunication systems, advanced radar systems, etc. An often-used method of characterizing MIMO antennas is to determine the correlation coefficient (ρ_{CC}) between the antennas [13, 14, 15, 16], which can be obtained through S-parameters measured in RC and anechoic chamber (AC) environments [4, 5, 17].

However, we do not know how the determination of ρ_{CC} is affected by loading in the RC environment. Therefore, the focus of this paper will be a comparison of ρ_{CC} of MIMO antennas under different loading configurations. Also, ρ_{CC} is compared with the standard S-parameter formulation in assessing spatial uniformity.

Similar to [5], the effect on ρ_{CC} of the separation between two parallel monopole antennas on a ground plane is studied. Two different loading configurations are considered by placing six RF absorber-sections in the far corners of the RC. The effect of spatial uniformity on ρ_{CC} is investigated by measurements at nine different positions in the RC.

Our study is intended to determine if 1) loading of the RC causes a sufficient change in the correlation coefficient such that real-world channel simulation in a RC is not possible for a MIMO system, and 2) either metric provides a means of establishing the field-uniformity in the RC.

II. MEASUREMENT SETUP

The measurements were all done in an RC at the National Institute of Standards and Technology in Boulder, Colorado. This RC has two mechanical stirrers which rotate stepwise. A pseudo-random grid [18] was used for the paddle angles to maximize the number of independent samples. The number of independent stirrer-states is not investigated explicitly, but is estimated (based on [18]) to be an order of magnitude smaller than the 1000 samples collected here. The independence of stirrer-states is a difficult topic and has several different approaches as mentioned in [19, 18]. With that stated, the number of stirrer-states used here is higher than strictly required. This is done to decrease the uncertainty in the estimate of ρ_{CC} , as will be explained in Section III.B.

A four-port vector network analyzer (VNA) was swept over the frequency band from 1.5 GHz to 2.5 GHz. The band was split into 4001 equidistant frequency points. Each point was measured after a sweep-dwell-time of 10 μ sec. The power specified on the VNA was kept constant during all the measurements and was set to -8 dBm. To describe what is meant by 'position' in our RC, a coordinate system is defined in Fig. 1 together with the dimensions of the RC, which are 4.27 m \times 3.65 m \times 2.9 m.

A. Antenna Specifications

The measurements were carried out with two similar types of monopole antenna arrays. All antennas were tuned to a resonance frequency of 1.9 GHz (or a wavelength of $\lambda = 15.78$ cm). The ground planes were made of aluminum and had a thickness of 1.6 mm. The ground plane dimensions are specified in Table I.

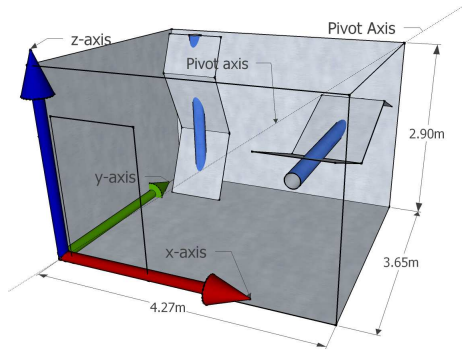


Figure 1. RC dimensions and the chosen coordinate system.

The first antenna has two variably-spaced parallel monopoles mounted on a ground plane. One of these monopoles stays fixed, while the other can be moved though a slot to vary the separation between the array's elements. This allows various values of antenna correlation. The opening of the slot was covered with metal tape to maintain the functionality. A second type of antenna with a fixed separation between the elements was also studied. All these antennas provided a range of correlation values, as well. They were placed in different positions to measure spatial uniformity and its effect on ρ_{CC} throughout the RC.

It was shown in [5, Figure 5] and [20] that increasing the separation of antenna elements results in decreasing correlation between them, thus increasing capacity. Therefore, a large separation (around $\lambda/2$ to λ) between the monopoles will be considered as a good MIMO antenna and monopoles with a small separation (smaller than $\lambda/2$) will be considered bad MIMO antennas. The separations for both types of antenna are summarized in Table II.

Table I
FIXED (F) AND VARIABLE (V) ANTENNA GROUND PLANE DIMENSIONS.

	Short (S) side	Long (L) side
F1	30.48 cm	30.48 cm
F2 to F4, and all V	30.48 cm	45.72 cm

Table II
FIXED (F) AND VARIABLE (V) ELEMENT SEPARATION DISTANCES.

Distance	Wavelength		Distance	Wavelength	
V1	15.08 cm	0.96λ	V7	6.27 cm	0.40λ
V2	14.21 cm	0.90λ	V8	4.76 cm	0.30λ
V3	12.62 cm	0.80λ	V9	3.18 cm	0.20λ
V4	11.03 cm	0.70λ	F3	3.16 cm	0.20λ
V5	9.45 cm	0.60λ	V10	1.67 cm	0.11λ
V6	7.86 cm	0.50λ	F2	1.55 cm	0.10λ
F4	6.28 cm	0.40λ	F1	1.00 cm	0.06λ

B. Loading of the Reverberation Chamber

As was shown in [21], loading decreases the spatial uniformity in a RC. In order to obtain an improved understanding

on the effect of decreasing spatial uniformity on ρ_{CC} as compared to complex transmission-coefficient S-parameters (S_{xy}), two loading configurations were used. One loading configuration used no absorbers, and one used six blocks of absorber stacked in the four corners of the RC. The far corners were used to minimize distortion of the antennas' near-field and radiation patterns. The dimensions of these absorbers are 60 cm \times 60 cm \times 60 cm and a portion of the top 40 cm of each absorber is removed to form nine distinct, equally sized pyramids.

Loading the RC is common practice for testing wireless devices, as it can create a more realistic wireless testing environment [8, 9]. The chamber decay time decreases when an RC is loaded, replicating some propagation environments well. However, too much absorber is a detriment to the chamber performance [21] and [22].

C. Positions in the Reverberation Chamber

To measure spatial uniformity and ρ_{CC} , three locations, described in Table III as L1 to L3, were chosen within the x, y -plane of the RC. At each location, the antenna elements were a distance of at least $\lambda/2$ from the floor, walls, ceiling and stirrers. The antennas were rotated to three different orientations about the pivot axis. This pivot axis is indicated as a dashed line in Fig. 1 going diagonally through the RC. Combining locations and orientations results in nine positions of the fixed antenna arrays.

Table III
THE LOCATIONS (L1 TO L3) IN THE RC FOR THE MONOPOLE ANTENNAS.

	Location (cm)		
	L1	L2	L3
X	180.3	218.4	58.4
Y	144.8	223.5	101.6
Z	108.0	205.7	20.3

III. ANALYSIS METHODS

In this section, the K-factor and spatial uniformity are obtained from the complex reflection-coefficient S-parameters (S_{xx}) and complex transmission-coefficient S-parameters (S_{xy}). The correlation coefficient is found from the stirred component (defined below) of S_{xy} , and ρ_{CC} is expressed as a squared (or power-like) quantity from the measurement of S_{xy} . Finally, the coefficient of variation (C_v) is used to compare both metrics for different loading configurations.

A. Complex Transmission and Reflection Coefficients Metrics

For each measurement, three ports of the four port VNA were used, two for the antenna arrays and one for the transmit antenna (a horn antenna). This resulted in nine S-parameters for each measurement. These S-parameters are complex numbers representing the reflected S_{xx} or transmitted S_{xy} waves. The subscript " xy " corresponds to the two ports used in a given VNA measurement.

The measured S_{xx} and S_{xy} in a paddle-stirred RC environment contain a stirred and an unstirred part. The stirred part is the part of the field that gets scattered by the stirrers, while the unstirred part contains the line-of-sight component and the reflections from the floor, ceiling or walls.

The stirred, unstirred, and total parts of S_{xy} are given as squared power-like quantities by the following:

$$\langle |S_{xy}^s|^2 \rangle = \langle |S_{xy} - S_{xy}^{us}|^2 \rangle = \langle |S_{xy} - \langle S_{xy} \rangle|^2 \rangle \quad (1)$$

$$\langle |S_{xy}^{us}|^2 \rangle = |\langle S_{xy} \rangle|^2 \quad (2)$$

$$\langle |S_{xy}^t|^2 \rangle = \langle |S_{xy}|^2 \rangle. \quad (3)$$

The $\langle \cdot \rangle$ indicates the ensemble average over the stirrer-state (a stirrer-state corresponds to a paddle position), the $|\cdot|$ indicates the complex magnitude value, the superscript "s" represents contributions from the stirred energy, "us" represents contributions from the unstirred energy and "t" represents contributions from the total energy of the S_{xy} .

The S-parameters given in (1) need to be corrected for the possibility of the use of mismatched antennas. A common way to correct S-parameters measurements made in an RC for antenna mismatch is to replace the S-parameter given above by the following (for more details see [23, 8])

$$\langle |S_{xy}|^2 \rangle \rightarrow \frac{\langle |S_{xy}|^2 \rangle}{(1 - |\langle S_{xx} \rangle|^2)(1 - |\langle S_{yy} \rangle|^2)}. \quad (4)$$

A common metric for assessing how well fields in the RC are stirred is the Rician K-factor. The K-factor gives the ratio between the stirred and unstirred part of the fields and is given by [8]

$$K = \frac{|\langle S_{xy} \rangle|^2}{\langle |S_{xy} - \langle S_{xy} \rangle|^2 \rangle} = \frac{\langle |S_{xy}^{us}|^2 \rangle}{\langle |S_{xy}^s|^2 \rangle}. \quad (5)$$

B. Correlation Coefficient

The calculation of the correlation coefficient is given by [24, Eq. 9]

$$\rho_{CC} = \frac{\left| \frac{\sum_s [(S_{x_1y} - \langle S_{x_1y} \rangle)(S_{x_2y} - \langle S_{x_2y} \rangle)^*]}{\sqrt{\sum_s |S_{x_1y} - \langle S_{x_1y} \rangle|^2} \sqrt{\sum_s |S_{x_2y} - \langle S_{x_2y} \rangle|^2}} \right|}{\left| \frac{\sum_s [(S_{x_1y} - \langle S_{x_1y} \rangle)(S_{x_2y} - \langle S_{x_2y} \rangle)^*]}{\sqrt{\sum_s |S_{x_1y} - \langle S_{x_1y} \rangle|^2} \sqrt{\sum_s |S_{x_2y} - \langle S_{x_2y} \rangle|^2}} \right|}. \quad (6)$$

The sub-subscripts (at the "x" subscripts) in the S-parameters indicate one of the two ports connected to the monopoles. As will be shown, the correlation coefficient (ρ_{CC}) can be calculated independent of the randomness of the field, that is, whether or not it is well stirred.

C. Coefficient of Variation

To assess how the ρ_{CC} metric compares to the classic S_{xy} power-like metric in assessing spatial uniformity when loading

the RC, the coefficient of variation (C_v) is used. As explained in [25, §3.1.3], the C_v is defined as

$$C_v = \frac{\sigma_p(x)}{\langle x \rangle_p}, \text{ where } x \in \left\{ \rho_{CC}, \langle |S_{xy}^s|^2 \rangle \right\} \quad (7)$$

which is simply the ratio of the sample standard deviation to the sample mean. The average $\langle x \rangle_p$ and the standard deviation (σ_p) are taken over N different positions, each indicated with the subscript "p". In this case, the sample standard deviation σ_p would be

$$\sigma_p(x) = \sqrt{\frac{1}{N-1} \sum_{p=1}^N (x - \langle x \rangle_p)^2}. \quad (8)$$

D. Measurement Uncertainty

For the different components of measurement uncertainty, the relative or fractional uncertainty will be used to relate to the uncertainty for this chamber previously found in [7]. The relative uncertainty is given by $u_x = \frac{\sigma_x}{\langle x \rangle}$. This quantity will be expressed on a logarithmic scale of the magnitude, and therefore $u_{x,\text{dB}} = 10 \log_{10} \left(\frac{\langle x \rangle - \sigma_x}{\langle x \rangle} \right)$ is used, in which $\langle x \rangle$ is the expected value of a process x , where we assume that x is a power-type quantity.

The uncertainties in the measurements are shown in Table IV (on the first row). They are based on the raw measured S_{xy} and S_{xx} values (without any mismatch correction or stirred energy estimations). The uncertainties are calculated for all antennas and the maximum of these values was selected.

The uncertainty of the VNA (u_{VNA}) needs to be considered as well. Since each measurement in this research had a two- or five-hour duration and a similar configuration as [7], the same uncertainty is considered a reasonable estimate, as well.

Table IV
RELATIVE VNA MEASUREMENT UNCERTAINTIES

Uncertainty source	No absorbers	Six absorbers
$u \sqrt{\langle S_{xx}^m ^2 \rangle}$	0.20 dB	0.39 dB
u_{VNA}	0.02 dB	0.02 dB
u_{Total}	0.20 dB	0.39 dB

Note that when calculating ρ_{CC} , an additional uncertainty arises. According to simulations done in [10, Fig. 2], for an $\rho_{CC} \geq 0.1$ this would result in an uncertainty of $u_{CC} \leq 1.2$ dB. However, this uncertainty is not a measurement uncertainty, but rather a computational variation in the estimation of ρ_{CC} . Therefore, this uncertainty is not included in the total measurement uncertainty.

IV. RESULTS

First, the spatial uniformity is assessed in the RC for both the loaded and unloaded cases. The K-factor is considered, as well as the C_v of the $\langle |S_{xy}|^2 \rangle$ and the ρ_{CC} .

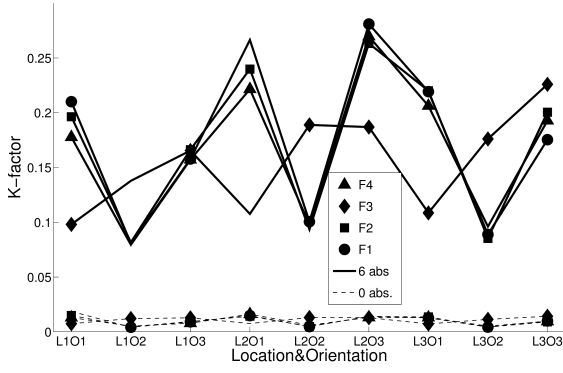


Figure 2. K-factor for all four fixed antennas with zero absorber (dashed) and six absorbers (solid) for all nine positions, averaged over frequency.

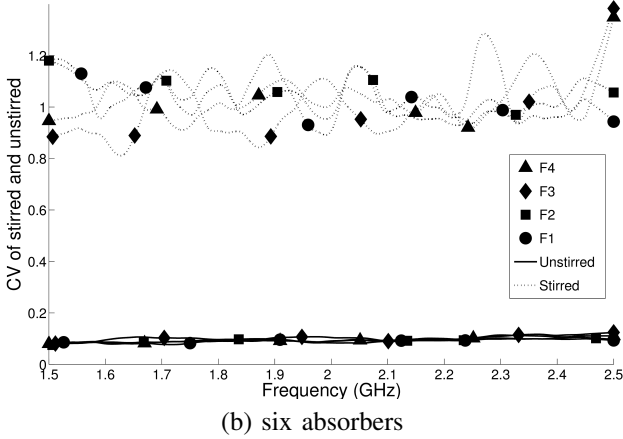
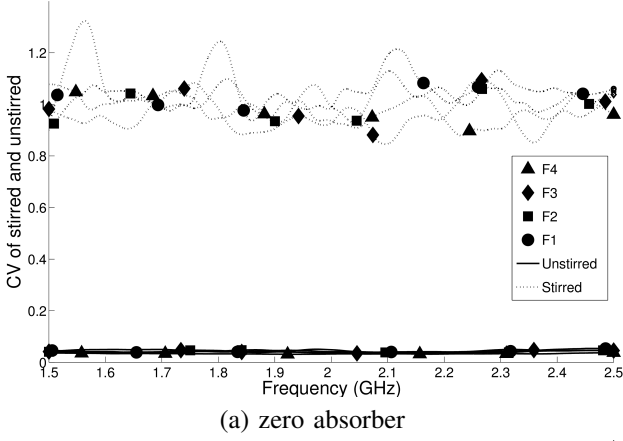


Figure 3. C_v of $\langle |S_{xy}|^2 \rangle$, for both the stirred (solid) and unstirred part (dotted). Both S_{xy} and S_{xx} are averaged over position for all four fixed antennas. The data are smoothed with a 400 point window (or a 0.1 GHz bandwidth).

A. Spatial Uniformity and Complex Transmission Coefficient

Fig. 2 shows the K-factor at each position (averaged over the frequency band) for all fixed antenna separations in two loading configurations. There is a clear difference between the two loading configurations. For the six-absorber-loading configuration, the K-factor varies between ~ 0.1 and 0.3 for all positions. For the unloaded case, the RC can be considered well stirred and more spatially uniform.

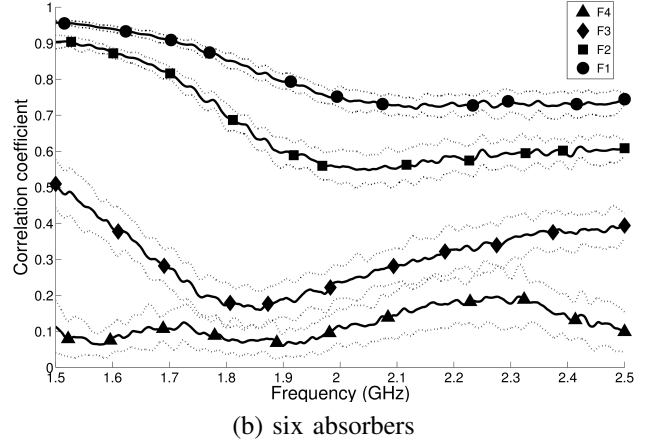
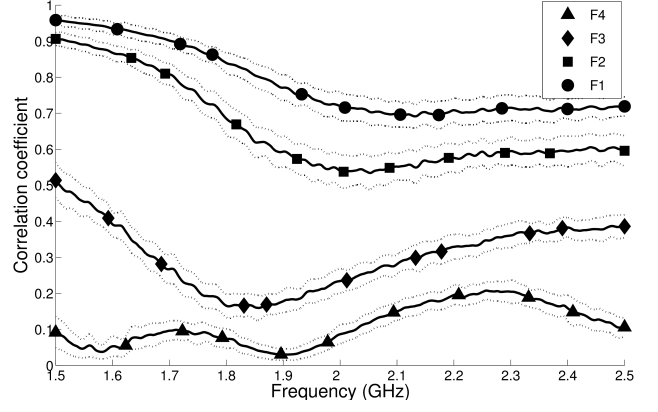


Figure 4. ρ_{CC} for the fixed separations averaged (solid) over all positions and with a 2σ spread (dotted). Both graphs are smoothed with a 100 point window (or a 0.1 GHz bandwidth).

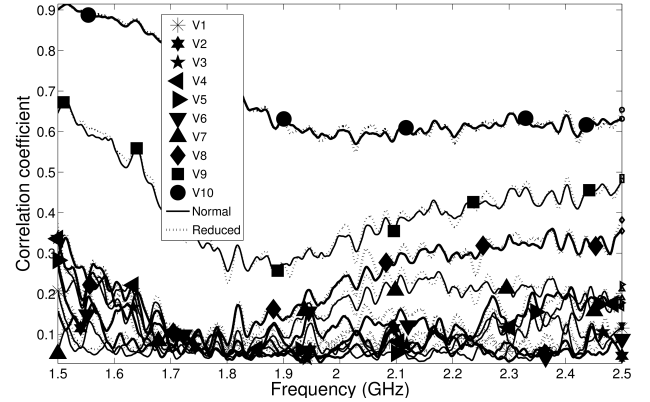


Figure 5. ρ_{CC} when the RC is loaded with six absorbers with $N = 1000$ (solid) with $N = 100$ (dotted) points for all variable separations. The graph is again smoothed with a 100 point window (or a 0.1 GHz bandwidth).

Fig. 3 shows C_v of $\langle |S_{xy}|^2 \rangle$ (its stirred and unstirred parts separately). The variation appears to be caused mainly by the unstirred part of this quantity. C_v of the unstirred part almost doubles when the RC is loaded, while C_v of the stirred part remains largely unchanged. Hence, the spatial uniformity in the RC decreases, as expected.

B. Correlation Coefficient

Fig. 4 shows ρ_{CC} averaged over the nine positions for the fixed-spacing antennas for the unloaded and loaded cases. There is little change in the 2σ bounds with loading. As well, the averages are similar, and the frequency response remains approximately the same.

In Fig. 5, the frequency response for the variable-separation monopoles is similar to the response shown for the fixed-separation antennas in Fig. 4. The unloaded case (not shown in Fig. 5) has a less irregular behavior for the frequency response compared to the loaded case.

Fig. 5 shows a more variable behavior if ρ_{CC} is calculated with fewer stirrer-states (dotted, with $N = 100$) than when all stirrer-states are used (solid, with $N = 1000$). This corresponds to the findings in [10]. Overall there is little difference in ρ_{CC} for the loaded and unloaded cases, even when the number of stirrer-states is artificially reduced.

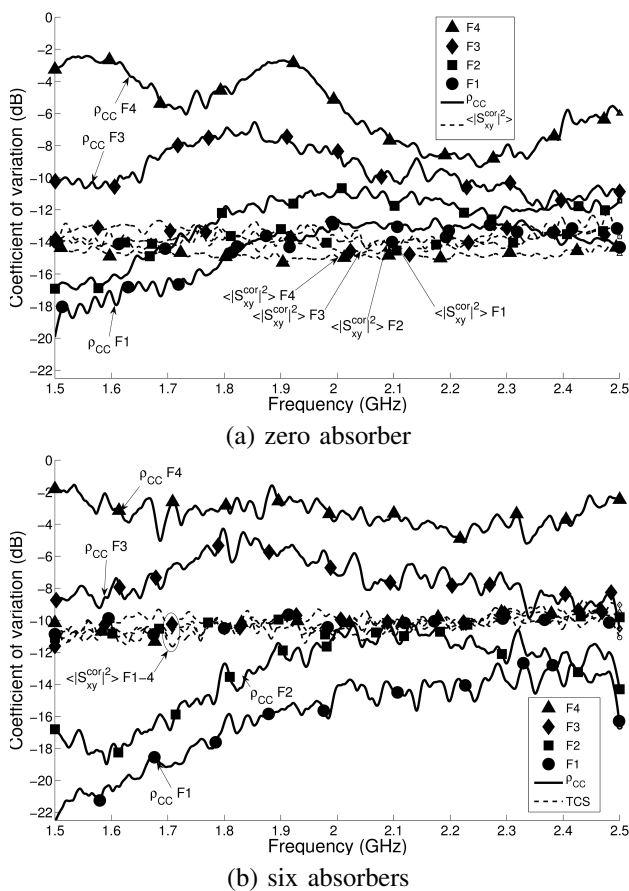


Figure 6. Coefficient of variation of ρ_{CC} (solid) and $\langle |S_{xy}|^2 \rangle$ (dashed) over all positions for the fixed antennas. A 100 point window (around 25 MHz) is used for smoothing.

C. Complex Transmission Coefficient and Correlation Coefficient Compared

In Fig. 6, C_v is computed over the positions for the four fixed separations for both ρ_{CC} (solid) and $\langle |S_{xy}|^2 \rangle$ s (dashed). In comparing Fig. 6(a) and Fig. 6(b), there are

several important features to note when the RC is loaded. First of all, C_v of $\langle |S_{xy}|^2 \rangle$ increases by approximately 3 dB overall, as was shown in Fig. 3. Because $\langle |S_{xy}|^2 \rangle$ is sensitive to loading, it is not a good metric to use for assessing the performance of MIMO antennas in a RC.

The ρ_{CC} for fixed separations 3 and 4 (the good MIMO antennas) flattens out, and on average there is just a minor increase with a peak of 2 dB around 2.2–2.3 GHz. Therefore, the ρ_{CC} metric becomes less accurate for these antennas as well, though in a far lesser amount than $\langle |S_{xy}|^2 \rangle$ does. The ρ_{CC} is less influenced by a decrease in spatial uniformity.

For fixed separations 1 and 2 something interesting occurs. These separations are less than 0.11λ and would thus qualify as bad MIMO antennas. For these two, however, ρ_{CC} becomes more accurate with loading as C_v overall decreases by values from 0.5 dB for separation 2 up to 2 dB for the lower frequency range of separation 1.

V. CONCLUSION

We found that ρ_{CC} can be found accurately in a loaded or unloaded RC environment, making it almost independent of spatial uniformity. The correlation coefficient values and corresponding coefficient of variation were not significantly different for the unloaded versus loaded RC measurements. This implies that "tuning" the RC to match real-world channel conditions; e.g., delay spread statistics, will not affect the measured correlation between the antenna elements in a MIMO antenna. This supports the use of a loaded RC to create real-world environments for the evaluation of wireless MIMO systems.

VI. ACKNOWLEDGMENT

The authors thank John Ladbury of NIST for his support in the reverberation chamber laboratory, and Ryan J. Pirkl (formerly a postdoctoral research fellow at NIST) for his help, patience and explanations. We also thank ETS-Lindgren for supplying the absorber blocks used in this work.

REFERENCES

- [1] M. Garcia-Fernandez, J. Valenzuela-Valdes, and D. Sanchez-Hernandez, "Latest advances in mode-stirred reverberation chambers for MIMO OTA evaluation of wireless communications devices," *Proceedings of the 5th European Conference on Antennas and Propagation (EUCAP)*, pp. 2427–2431, 2001.
- [2] D. Kurita, Y. Okano, S. Nakamatsu, and T. Okada, "Experimental comparison of MIMO OTA testing methodologies," in *Antennas and Propagation (EuCAP), 2010 Proceedings of the Fourth European Conference on*, april 2010, pp. 1–5.
- [3] X. Chen, P.-S. Kildal, J. Carlsson, and J. Yang, "Comparison of Ergodic Capacities From Wideband MIMO Antenna Measurements in Reverberation Chamber and Anechoic Chamber," *IEEE Antennas Wireless Propag. Lett.*, vol. 10, pp. 446–449, 2011.
- [4] K. Rosengren, P. Bohlin, and P.-S. Kildal, "Multipath characterization of antennas for MIMO systems in reverberation chamber including effects of coupling and efficiency," in *Antennas and Propagation Society International Symposium, 2004. IEEE*, vol. 2, June 2004, pp. 1712–1715 Vol.2.
- [5] P.-S. Kildal and K. Rosengren, "Correlation and capacity of MIMO systems and mutual coupling, radiation efficiency, and diversity gain of their antennas: simulations and measurements in a reverberation

- chamber," *IEEE Commun. Mag.*, vol. 42, no. 12, pp. 104–112, Nov. 2004.
- [6] Q. He and R. Blum, "Diversity Gain for MIMO Neyman-Pearson Signal Detection," *IEEE Trans. Signal Process.*, no. 3, pp. 869–881, March.
- [7] C. L. Holloway, H. Shah, R. Pirkl, W. Young, D. Hill, and J. Ladbury, "Reverberation Chamber Techniques for Determining the Radiation and Total Efficiency of Antennas," *IEEE Trans. Antennas Propag.*, vol. 60, no. 4, pp. 1758–1770, April 2012.
- [8] C. L. Holloway, D. Hill, J. Ladbury, P. Wilson, G. Koepke, and J. Coder, "On the Use of Reverberation Chambers to Simulate a Rician Radio Environment for the Testing of Wireless Devices," *IEEE Trans. Antennas Propag.*, vol. 54, no. 11, pp. 3167–3177, Nov. 2006.
- [9] E. Genender, C. L. Holloway, K. Remley, J. Ladbury, G. Koepke, and H. Garbe, "Simulating the Multipath Channel With a Reverberation Chamber: Application to Bit Error Rate Measurements," *IEEE Trans. Electromagn. Compat.*, vol. 52, no. 4, pp. 766–777, Nov. 2010.
- [10] P. Hallbjörner, "Accuracy in Reverberation Chamber Antenna Correlation Measurements," in *Antenna Technology: Small and Smart Antennas Metamaterials and Applications, 2007. IWAT '07. International Workshop on*, March 2007, pp. 170–173.
- [11] S. Floris, K. Remley, and C. L. Holloway, "Bit Error Rate Measurements in Reverberation Chambers Using Real-Time Vector Receivers," *IEEE Antennas Wireless Propag. Lett.*, vol. 9, pp. 619–622, 2010.
- [12] K. Remley, H. Fielitz, H. Shah, and C. L. Holloway, "Simulating MIMO techniques in a reverberation chamber," in *Electromagnetic Compatibility (EMC), 2011 IEEE International Symposium on*, Aug. 2011, pp. 676–681.
- [13] G. J. Foschini and M. L. Gans, "On limits of wireless communications in a fading environment when using multiple antenna," in *Wireless Personal Communications*, vol. 6, 1998, pp. 311–335.
- [14] D. Chizhik, G. J. Foschini, M. L. Gans, and R. A. Valenzuela, "Keyholes, Correlations, and Capacities of Multielement Transmit and Receive Antennas," *IEEE Trans. Wireless Commun.*, vol. 1, no. 2, pp. 361–368, Feb. 2002.
- [15] A. Farkasvolgyi, R. Dady, and L. Nagy, "Effect of Antenna Space on MIMO Channel Capacity in Practicable Antenna Structures," in *Progress in Electromagn. Research Symp., Moscow, Russia*, Aug. 18–21 2009, pp. 1065–1068.
- [16] C. Votis, G. Tatsis, and P. Kostarakis, "Envelope correlation parameter measurements in a MIMO antenna array configuration," in *Int. J. Commun. Network and System Sciences*, vol. 3, 2010, pp. 350–354.
- [17] K. Rosengren and P.-S. Kildal, "Radiation efficiency, correlation, diversity gain and capacity of a six-monopole antenna array for a MIMO system: theory, simulation and measurement in reverberation chamber," in *IEE Proceedings: Microwave, Antennas, and Propag.*, vol. 152, no. 1, 2005, pp. 7–16.
- [18] R. Pirkl, K. Remley, and C. Patane, "Reverberation chamber measurement correlation," *Electromagnetic Compatibility, IEEE Transactions on*, vol. 54, no. 3, pp. 533–545, June 2012.
- [19] C. Lemoine, P. Besnier, and M. Drissi, "Advanced method for estimating number of independent samples available with stirrer in reverberation chamber," *Electronics Letters*, vol. 43, no. 16, pp. 861–862, Feb. 2007.
- [20] M. Chiani, M. Win, and A. Zanella, "On the capacity of spatially correlated MIMO Rayleigh-fading channels," *Information Theory, IEEE Transactions on*, vol. 49, no. 10, pp. 2363–2371, Oct. 2003.
- [21] G. v. d. Beek, K. Remley, C. L. Holloway, J. Ladbury, and F. Leferink, "Characterizing Large-Form-Factor Devices in a Reverberation Chamber," *EMC Europe 2013*.
- [22] C. L. Holloway, D. Hill, J. Ladbury, and G. Koepke, "Requirements for an effective reverberation chamber: unloaded or loaded," *IEEE Trans. Electromagn. Compat.*, vol. 48, no. 1, pp. 187–194, Feb. 2006.
- [23] J. Ladbury, G. Koepke, and D. Camell, "Evaluation of the NASA Langley Research Center Mode-Stirred Chamber Facility," National Institute of Standards and Technology, Technical Note, Jan. 1999.
- [24] P.-S. Kildal and K. Rosengren, "Electromagnetic analysis of effective and apparent diversity gain of two parallel dipoles," *IEEE Antennas Wireless Propag. Lett.*, vol. 2, no. 1, pp. 9–13, 2003.
- [25] L. Arnaut, "Measurement uncertainty for reverberation chambers - I. Sample statistics." National Physical Laboratory, Hampton Road Teddington Middlesex United Kingdom, Report 2, Dec. 2008.